Applied Acoustics 190 (2022) 108640

Contents lists available at ScienceDirect

Applied Acoustics

journal homepage: www.elsevier.com/locate/apacoust

Cross-correlation quasi-gradient Doppler estimation for underwater acoustic OFDM mobile communications

Bin Li [a,b], Feng Tong [b,*], Jiang-hui Li [c], Si-yuan Zheng [b]

[a] Key Laboratory of Underwater Acoustic Communication and Marine Information Technology of the Minister of Education, Xiamen University, Xiamen, China
[b] College of Ocean and Earth Sciences, Xiamen University, Xiamen, China
[c] National Oceanography Centre Southampton, University of Southampton, Southampton, UK

ARTICLE INFO

Article history:
Received 10 April 2021
Received in revised form 28 December 2021
Accepted 11 January 2022
Available online 30 January 2022

Keywords:
Cross-correlation quasi-gradient (CCQG)
Doppler estimation
Orthogonal Frequency Division Multiplexing (OFDM)
Underwater acoustic communications

ABSTRACT

Orthogonal Frequency Division Multiplexing (OFDM) has drawn comprehensive attention due to its capability of achieving high data rate and high spectrum efficiency in underwater acoustic communications. However, the widespread Doppler effect in underwater acoustic channel caused by mobile vehicles or time varying medium can lead to significant distortion and deteriorate the demodulation performance, thus Doppler estimation and compensation are needed for OFDM mobile communications. Generally Doppler effect can be accurately estimated by calculating the dominant correlation-peak or cross-ambiguity function (CAF) between received and transmitted signals. However, this type of method is computationally intensive because of the exhausting search on the two-dimensional (2D) delay and Doppler compression factor space, thus unsuitable for small underwater vehicles that equipped with limited computational payload. In this paper, quasi-gradient of cross-correlation is defined to derive the cross-correlation quasi-gradient (CCQG) iterative estimation algorithm to achieve low complexity Doppler estimation. Moreover, the smoothed quasi-gradient and variable Doppler interval are employed to accelerate the convergence rate as well as to avoid being trapped at a local maximum. Numerical simulations and mobile communication sea trial experiments demonstrate the effectiveness and robustness of the proposed algorithm by comparing to the conventional cross-correlation estimation, auto-correlation estimation, block estimation and BER search estimation strategies.

1. Introduction

As the main tool of underwater wireless information transmission, the underwater acoustic communication technology has been undoubtedly expected to enable multifarious potential applications, such as marine environment monitoring, underwater exploitation, submarine pipe network laying and maintenance, disaster prevention and submarine assisted navigation [1,2,3,4,5]. Therefore, the transmission efficiency and robustness of underwater acoustic communications was emphasized due to the dramatically growing demand for transmitting, storing and managing the big maritime data [6,7,8].

The technology of Orthogonal Frequency Division Multiplexing (OFDM) has drawn significant attention in underwater acoustic communications due to its capability of achieving high data transmission rate and high spectrum efficiency [9,10,11]. However, the complicated characteristics of marine environment including tide, turbulence, wave and boundary effect generate adverse underwater acoustic channel which brings significant restrictions such as fast time-varying, severe fading, multipath, limited bandwidth and background noise [12,13,14,15,16]. Specially, recent years the rapidly increasing of research interests in underwater vehicles such as autonomous underwater vehicle (AUV), unmanned underwater vehicle (UUV) and glider, which also pose significant challenges for OFDM mobile communication at the presence of obvious Doppler effect and limited computational payload.

Particularly, for widespread Doppler, it would cause the destruction of orthogonality in OFDM, which may lead to significant distortion in received signal and degrade the demodulation performance severely [17,18]. Therefore, it is essential to estimate and compensate Doppler accurately for achieving stable OFDM communication performance.

Doppler effect on the received packets can be formulated as time compression or dilation, which will result in the accumulation of symbolic synchronization errors [19]. Therefore, especially for mobile underwater acoustic communications with high data rate, the Doppler estimation and compensation are needed to eliminate

* Corresponding author.
E-mail address: ftong@xmu.edu.cn (F. Tong).

https://doi.org/10.1016/j.apacoust.2022.108640
0003-682X/

the influence of Doppler on the demodulation performance of the receiver. Consequently, Doppler estimation becomes a key factor in the design of underwater acoustic OFDM communication systems.

Many Doppler estimation approaches have been utilized in underwater acoustic communications. A typical method [20] is that two Doppler-insensitive Linear frequency modulation (LFM) signals are inserted to the data frame in advance, and then the correlation detection is performed to acquire the variation of time difference between the first and last correlation peaks, which can be transformed into the Doppler factor. Subsequently a modified algorithm [21] based on this approach has been proposed and investigated, but the estimation accuracy of these algorithms will drop sharply at the presence of diffuse multipath propagation.

By measuring the frequency deviation of single frequency signals inserted in the data frame between the received signals and the transmitted packets, an efficient method for Doppler estimation was proposed and investigated [22]. Nevertheless, this strategy will experience performance degradation when frequency selective fading impairs the single frequency signals.

The single-branch auto-correlation (SBA) strategy has been extensively investigated to acquire Doppler factor by evaluating the period changes of periodic transmitted signal [23,24]. Even though it possesses low computational complexity, it cannot be applied to the scenarios containing acceleration. To make it more applicable, a multi-branch auto-correlation (MBA) algorithm [25] was proposed, which is capable of addressing underwater acoustic channels associated with fast moving and manoeuvring vehicles. Compared to the cross-correlation based methods, such auto-correlation methods are more robust against multipath especially at high SNRs [26].

In terms of the frequency calculation for Doppler estimation, some novel mathematical methods are also introduced instead of the classic Fourier transform, including the fractional Fourier transform (FRFT) [27] and partial fast Fourier transform (P-FFT) [28] with the purpose to improve accuracy and reduce complexity. Nevertheless, the estimation accuracy of these algorithms significantly degrades with large-scale Doppler caused by high-speed motion between the transmitter and receiver.

A minimum bit error rate (BER) based principal for Doppler estimation is investigated to transform the signal-level Doppler estimation into a bit-level search [29]. Similarly, as an adaptive version of the BER search approach, a super-resolution, yet low-complexity algorithm based on stochastic gradient has been proposed to address long multipath and severe Doppler fluctuations [30]. Nonetheless, this type of estimation approach based on bit error information is required to contain the demodulation process in Doppler estimation.

Previous investigations indicated that the classic cross-correlation estimation algorithm based on evaluating the dominant correlation-peak (determined by cross-correlation function, CCF) or cross-ambiguity function (CAF) between transmitted and received packets is capable of achieving high estimation accuracy [31,32]. However, as the position of maximum correlation-peak or CAF magnitude is obtained by exhaustively searching in a two-dimensional grid of delays and Doppler factors, massive amounts of searching grids will lead to intensive computation complexity.

To reduce computational complexity in cross-correlation estimation strategy, a two-step approach (coarse estimation and fine estimation) was proposed and investigated, which reduces the number of Doppler grids and accelerates computation [33]. Nonetheless, even though the searching interval is small, it can still result in considerable computational overhead in the fine estimation stage, especially for practical hardware implementation.

Different from the common stochastic gradient algorithm, stochastic quasi-gradient algorithm [34] generalizes the stochastic approximation approach with unconstrained optimization of the expectation of a random function to solve the general constraints and non-differentiable, non-convex functions, thus it can be utilized for such optimization problems where gradient does not exist or function is non-convex. Due to the above advantages, it has been generally applied to solve multifarious stochastic optimization problems, such as dynamic traffic assignment [35], chemical dynamics in closed systems [36] and voltage control of electricity distribution networks [37].

A new algorithm named gradient orientation selective cross-correlation was proposed for image matching, which indicated the CCF near the dominant correlation-peak can be regarded as a convex-like function when applying cross-correlation strategy for Doppler estimation [38]. Motivated by this, in this paper we propose a novel low-complexity Doppler estimation algorithm by transforming the cross-correlation based Doppler estimation into a problem of stochastic quasi-gradient optimization. Specifically, after the dominant correlation-peak area is ascertained by the conventional coarse Doppler estimation, the fine Doppler search is performed iteratively along the quasi-gradient direction. Moreover, the smoothed quasi-gradient and variable Doppler interval are adopted to accelerate the convergence rate and avert the unacceptable convergence to the local optimization. The effectiveness and robustness of the proposed strategy are then demonstrated by numerical simulations and sea trial experiments, compared to the conventional cross-correlation estimation [31], auto-correlation estimation [39,40], block estimation [20] and BER search estimation [29] algorithms.

The contributions of this paper are listed as follows. First, by converting the problem of Doppler searching estimation on the two-dimensional delay and Doppler compression factor space into that of stochastic quasi-gradient optimization, the cross-correlation quasi-gradient (CCQG) is defined to derive a type of iterative estimation algorithm for achieving much less complexity Doppler estimation, thus it can be especially suitable for small underwater vehicles which equipped with limited computational overhead in various marine missions. Second, two constraints including the smoothed quasi-gradient and variable Doppler interval are designed for accelerating the convergence rate and reducing the possibility of local optimization. Moreover, the impact of algorithm parameters on estimation performance, the computational complexity and convergence are evaluated in detail.

The rest of this paper is organized as follows. In Section 2, the signal model, Doppler estimation algorithms and some constrained conditions are introduced. The experimental results and the analysis of computational complexity and convergence are suggested in Section 3. Conclusions are summarized in Section 4.

2. Model and algorithm

2.1. Cross-correlation estimation algorithm

The transmitted signal of cyclic-prefixed (CP) OFDM blocks can be formulated as

$$s(t) = \Re\left\{ e^{j2\pi f_c t} \sum_{k=-L/2}^{L/2-1} D_k e^{j2\pi \frac{k}{T_s} t} g(t) \right\} \tag{1}$$

where f_c represents the center frequency, D_k denotes the k-th sub-carrier symbol in the OFDM symbol, T_s is the basic OFDM symbol duration, L denotes the number of sub-carriers, and $g(t)$ is defined as a rectangular window which includes the CP and one basic OFDM symbol duration given by

$$g(t) = \begin{cases} 1, & t \in [-T_{cp}, T_s] \\ 0, & \text{otherwise} \end{cases} \tag{2}$$

where T_{cp} denotes the length of the CP.

The underwater acoustic channel can be formulated as a time-varying linear system with an impulse response given by

$$h(t,\tau) = \sum_p A_p(t)\delta(\tau - \tau_p(t)) \tag{3}$$

where $A_p(t)$ and $\tau_p(t)$ represent the time-varying amplitude response and delay of the p-th path, respectively.

Suppose a common Doppler factor σ such that $\tau_p(t) = \tau_p - \sigma t$ and further assume the p-th amplitude response experiences slow variation such that $A_p(t) \approx A_p$ for the duration of one OFDM block, (3) can be rewritten as

$$h(t,\tau) = \sum_p A_p \delta(\tau - \tau_p + \sigma t) \tag{4}$$

Though in (3) all the paths are assumed to have a common Doppler factor, in practice some paths may experience different Doppler factors. To simplify the derivation, this type of different path can be equivalently assumed as additive noise. Note that, so long as the dominant Doppler is caused by the direct motion between transmitter and receiver, the common Doppler factor assumption can be applied without the loss of generality [41].

Based on the above basic premises, the received OFDM symbol can be formulated as

$$\tilde{r}(t) = \Re\left\{\sum_p A_p e^{j2\pi f_c(t+\sigma t-\tau_p)}\left[\sum_{k=-L/2}^{L/2-1} D_k e^{j2\pi\frac{k}{T_s}(t+\sigma t-\tau_p)} g(t+\sigma t-\tau_p)\right]\right\} + \tilde{n}(t) \tag{5}$$

where $\tilde{n}(t)$ represents the additive white Gaussian noise.

Thus, the baseband version $r(t)$ of $\tilde{r}(t)$ can be formulated as

$$r(t) = \sum_{k=-L/2}^{L/2-1}\left\{D_k e^{j2\pi\frac{k}{T_s}t} e^{j2\pi\sigma f_k t}\left[\sum_p A_p e^{-j2\pi f_k \tau_p}\right] g(t+\sigma t-\tau_p)\right\} + n(t) \tag{6}$$

where $n(t)$ denotes the baseband white Gaussian noise, and f_k represents the frequency of the k-th sub-carrier given by

$$f_k = f_c + k/T_s, \quad k = -\frac{L}{2}, -\frac{L-1}{2}, \ldots, \frac{L}{2} - 1 \tag{7}$$

For the continuous stationary signal, its ambiguity function (AF) can be defined as [42]

$$\Psi(\tau,\sigma) = \sqrt{1+\sigma}\int_{-\infty}^{\infty} s((1+\sigma)t)s^*(t-\tau)dt \tag{8}$$

Moreover, the CAF can be formulated as

$$\Psi^*(\tau,\sigma) = \sqrt{1+\sigma}\int_{-\infty}^{\infty} s((1+\sigma)t)r^*(t-\tau)dt \tag{9}$$

Suppose that τ is set to zero, the Doppler estimation approach utilizing the CAF should be modified as

$$\sigma = \underset{\sigma\in(\sigma_1,\sigma_2)}{\operatorname{argmax}}\{\Psi^*(0,\sigma)\} \tag{10}$$

where (σ_1, σ_2) represents the searching range of Doppler factor. Ultimately, the desired Doppler shift can be written as

$$\varepsilon = \sigma f_c \tag{11}$$

The CCF can be formulated as

$$\kappa(\varepsilon) = \max\left\{\left|s(t) \otimes r(t)e^{-j2\pi\varepsilon(0,1,\ldots,L_r-1)/f_s}\right|\right\} \tag{12}$$

where L_r denotes the length of $r(t)$, f_s represents the sampling rate, and $\otimes$ is defined as correlation operation. Thus, the Doppler estimation formula via the CCF can be given by

$$\varepsilon = \underset{\varepsilon\in(\varepsilon_1,\varepsilon_2)}{\operatorname{argmax}}\{\kappa(\varepsilon)\} \tag{13}$$

where $(\varepsilon_1, \varepsilon_2)$ denotes the searching range of Doppler.

From (9), (10), (12) and (13) one may notice that the cross-correlation strategy is actually implemented in the form of multiple correlators, each of which performs cross-correlation between received signal and transmitted signal with different Doppler to produce an associated correlation-peak. The desired Doppler can be determined by searching the largest magnitude of correlation-peak. However, this type of exhaustive search will lead to an extremely high computational complexity when a small search interval is used to ensure high accuracy.

2.2. The proposed CCQG algorithm

In this section, we proposed an algorithm to formulate the Doppler estimation with iterative quasi-gradient optimization. Firstly the region of dominant correlation-peak, namely the coarse searching window of Doppler, can be initially determined by (12) and (13). Subsequently, different from the direct search strategy that yields high accuracy with small searching interval, the quasi-gradient of CCF is adopted to derived a low complexity iterative searching algorithm.

The quasi-gradient of CCF δ is defined as

$$\delta = \kappa(\varepsilon + \Delta\varepsilon_f) - \kappa(\varepsilon) \tag{14}$$

where $\Delta\varepsilon_f$ represents the fine Doppler searching interval, the selection of which will be interpreted later. Subsequently, the Doppler search can be recursively adapted by the quasi-gradient iteration as

$$\underset{\varepsilon\in(\varepsilon_b,\varepsilon_e)}{\kappa(\varepsilon_n+1)} = \kappa(\varepsilon_n) + \delta_n \tag{15}$$

where δ_n denotes the step-size of quasi-gradient iteration, and $(\varepsilon_b, \varepsilon_e)$ is the coarse searching window of Doppler, which is determined by the conventional coarse Doppler estimation.

Similar to the classic gradient optimization scenario where a single global optimum cannot be theoretically guaranteed, herein the $\kappa(\varepsilon)$ may convergence to a local maximum other than the global optimum one. Therefore, we employ several constrains to avoid this undesired result [43].

First, instead of the original quasi-gradient of CCF in (14), the smoothed quasi-gradient is introduced to reduce the possibility of local maximums, which is given by

$$\bar{\delta}_n = \frac{1}{\lambda}\sum_{i=n-\lambda+1}^{n}\delta_i \tag{16}$$

where λ is the length of smoothing window. Thus (15) can be modified as

$$\underset{\varepsilon\in(\varepsilon_b,\varepsilon_e)}{\kappa(\varepsilon_n+1)} = \kappa(\varepsilon_n) + \bar{\delta}_n, \quad \bar{\delta}_n \geq 0 \tag{17}$$

To accelerate the optimization, $\Delta\varepsilon_f$ is designed to decrease gradually according to the times of negative $\bar{\delta}_n$ during the iterations as

$$\Delta\varepsilon_f = \begin{cases} 2^{-\mu}, & 0 \leq \mu < M \\ v, & \mu \geq M \end{cases} \tag{18}$$

where μ denotes the times of negative $\bar{\delta}_n$ in the process of optimization, v represents the resolution of fine Doppler searching interval, and M is the judgement threshold. Note that, $\mu = 0$ indicates that the initial $\Delta\varepsilon_f$ is set to 1.

As a result, the Doppler estimation equation via CCQG algorithm can be formulated as

$$\hat{\varepsilon} = \underset{\varepsilon\in(\varepsilon_n-\lambda,\varepsilon_n-1)}{\operatorname{argmax}} \{\kappa(\varepsilon)\} \tag{19}$$

where $\varepsilon \in (\varepsilon_n - \lambda, \varepsilon_n - 1)$ represents the final Doppler search window determined by (17).

From the above derivation, Doppler estimation is transformed into the quasi-gradient iterative optimization. By adopting the smoothed quasi-gradient and variable Doppler interval, the proposed strategy is capable of achieving the trade-off between computational complexity and estimation precision. Moreover, the computational complexity and convergence of the CCQG algorithm will be investigated and analyzed in Section 3.4. The pseudo code of the proposed CCQG algorithm is described in Table 1.

2.3. Brief discussion about algorithm parameters

As revealed in Section 2.2, we introduce two constraints to guarantee the convergence toward the global optimization and thus reduce the computational complexity. Some brief discussions about the choices of the algorithm parameters are given as follows.

The length of smoothing window: a large λ can reduce the possibility of being trapped at the local maximum to solve the optimization. Nevertheless, as shown in (17), a large λ will increase computational complexity and decrease the convergence rate. Hence, the value of λ should be determined to seek a trade-off.

The fine Doppler interval: the parameter $\Delta\varepsilon_f$ determines the convergence rate and estimation precision. The sequential updating of $\Delta\varepsilon_f$ is derived in (18) to attain the optimum value by utilizing the times of negative smoothed quasi-gradient during the optimization.

The resolution of fine Doppler searching interval: a small v will increase the number of Doppler search. However, it does not guarantee the improvement of demodulation performance due to the possible mismatch between bit-level demodulation and the signal-level match of correlation [16]. As a consequence,v is determined by the trade-off between estimation precision and optimization speed.

Table 1
Pseudo code of the proposed CCQG algorithm.

Initialization settings ε_1, ε_2, λ,$\Delta\varepsilon_f$

(a) Updating the coarse searching window of Doppler.
Run (13) and modify the coarse searching window of Doppler as $(\varepsilon_b, \varepsilon_e)$.
(b) Running the CCF.
Run (12) using $\Delta\varepsilon_f$.
(c) Detecting whether $\bar{\delta}_n$ is positive or negative.
Compute $\bar{\delta}_n = \frac{1}{\lambda}\sum_{i=n-\lambda+1}^{n}\delta_i$.
If it is greater than or equal to 0, run (d).
If it is less than 0, $\mu = \mu + 1$ and run (e).
(d) Updating the Doppler searching function.
Run (17) using $\bar{\delta}_n$ and go back to the Step (b).
(e) Determining and updating the fine Doppler interval.
Compute $\Delta\varepsilon_f = \begin{cases} 2^{-\mu}, & 0 \le \mu < M \\ v, & \mu \ge M \end{cases}$
If it is greater than v, update $\Delta\varepsilon_f$ and go back to the Step (b).
If it is less than v, run (f).
(f) Solving the optimum Doppler.
Run (19) with n acquired by the Step (d).
(g) Output.
Solution of $\hat{\varepsilon}$.

3. Experiments and discussions

3.1. Numerical simulations

In this section, we apply numerical simulations to evaluate the performance of the proposed algorithm, with the conventional cross-correlation estimation, auto-correlation estimation, block estimation as well as BER search estimation methods as a comparison reference. The frame structure of the transmitted packet is illustrated in Fig. 1, with the parameters of which provided in Table 2. It can be observed that, while two Linear Frequency Modulation (LFM) signals are inserted before and after the data frame respectively for block estimation, a Doppler estimation signal consisted of two continuous OFDM symbols is placed in the beginning of data frame for cross-correlation estimation, auto-correlation estimation, BER search estimation and the proposed algorithm.

The length of smoothed window λ is set to 2. The coarse Doppler searching interval $\Delta\varepsilon_c$ which can be applied to evaluate the region of dominant correlation-peak is set to 2 Hz, and the fine Doppler searching interval $\Delta\varepsilon_f$ is set to 1 Hz corresponding to $\mu = 0$ at the initial stage. The parameter v is set to 0.01 Hz, and M is set to 4. The detailed configurations of the simulation system are provided in Table 2.

A typical underwater multipath channel is adopted for numerical simulation, incorporating direct path, surface reflected path and surface-bottom-surface reflected path, corresponding to the dominant coefficients associated with the magnitude of 0.76, 0.53 and 0.37 respectively [44,45]. The other coefficients are all set to zero to generate the channel response as presented in Fig. 2. The total multipath delay of it is 10 ms, which is consistent with the scale of some experimental scenarios. The additive white Gaussian noise and passband noise are employed to generate signal-to-noise ratio (SNR) from 0 dB to 10 dB and from 6 dB to

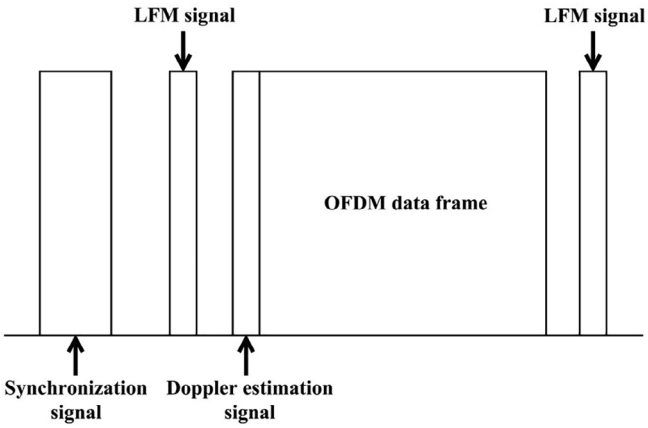

Fig. 1. The frame structure of transmitted signal.

Table 2
Parameters of transmitted packet.

Description	Value	Description	Value
Modulation mode	DQPSK	OFDM symbol duration (ms)	54.6
Center frequency (Hz)	15,500	Length of guard interval (ms)	13.65
Bandwidth (Hz)	5000	FFT points	4096
Sampling frequency (Hz)	75,000	Length of LFM signal (ms)	22.67
Number of sub-carrier	268	Length of Doppler estimation signal (ms)	136.6
Interval of sub-carrier (Hz)	18.3	Original communication rate (kbps)	3.93
Length of OFDM data frame (ms)	2048	Effective communication rate (kbps)	1.96

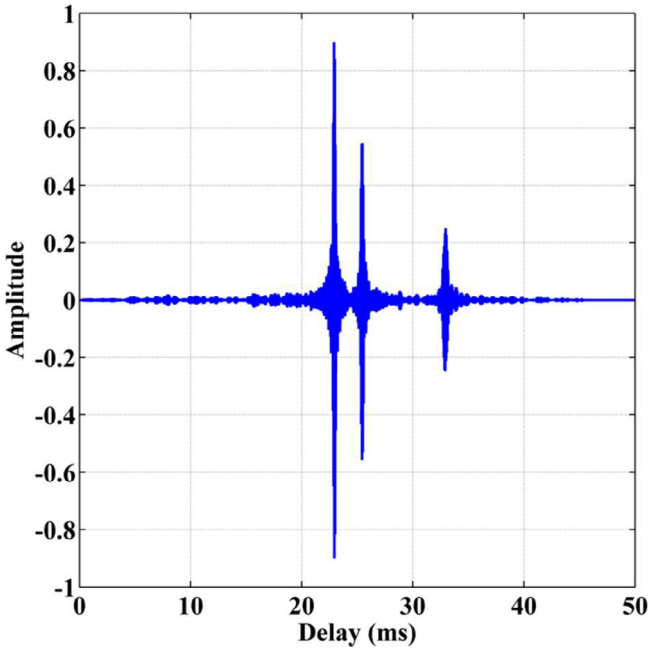

Fig. 2. Channel response of the simulation channel.

16 dB at the interval of 1 dB respectively. Furthermore, a Doppler of −8.5 Hz is artificially produced by resampling to simulate Doppler effects in the channel.

As the classic time–frequency differential OFDM receiver [46] directly utilizes the phase differences between both adjacent symbols and adjacent sub-carriers for differential detection thus no channel estimation and equalization are needed. To facilitate the evaluation of Doppler estimation performance, a classic time–frequency differential OFDM receiver as shown in Fig. 3 is adopted to perform OFDM demodulation after Doppler correction according to the Doppler estimates.

The Doppler estimation results under different background noise conditions acquired by the five approaches are provided in Fig. 4(a), from which we can see that the Doppler evaluated by block estimation is independent from the SNR and remains at about −8.95 Hz in the case of Gaussian noise and passband noise, while the Doppler curves of the other strategies exhibit slight variations within the range from −8.6 Hz to −8 Hz with respect to different SNRs.

As revealed in the BER curves shown in Fig. 4(b), BER curves of all the five Doppler estimated algorithms tend to decrease with the increasing of SNR at two types of noise. In the case of Gaussian noise, the cross-correlation estimation, BER search estimation and the CCQG approaches achieve similar performance, which are slightly better than the auto-correlation estimation and block estimation strategies in the conditions of low SNR. The cross-correlation estimation, auto-correlation estimation and the CCQG algorithm achieve similar estimation accuracy, which are slightly better than the block approach at the condition of passband noise. Moreover, the BER search strategy achieves the optimal estimation performance, because it can mitigate the mismatch between signal-level estimation and bit-level demodulation. The computational complexity of the proposed algorithm will be analyzed in Section 3.4 for further evaluation.

3.2. Sea trial

The sea trial data were collected from a mobile underwater acoustic communication scenario in a shallow water acoustic channel with gentle breeze and slight sea condition near the Xiamen Harbor, Xiamen, Fujian Province, China. The average depth of experimental area is about 10 m with the type of mud sea floor and semi-diurnal tide. Moreover, the tidal current exhibits the type of a reciprocating flow. The horizonal omni-directivity piezoelectric transducer was used as the sound source and receiver. With a source level of 185 dB re 1 μPa at 1 m and a receiving sensitivity level of −195 dB re 1 v/μPa, the cylindrical transducer has a diameter of 6.9 cm and a height of 10.9 cm.

Driven by a transmission power of 50 W, the transmitting transducer was towed at the depth of 3 m by a surface vessel moving towards an anchored surface vessel at a speed of 4–5 m/s. The receiving transducer was suspended under the anchored vessel at the depth of 3 m. A sound velocity profiler with the model HY1201 was used for collecting sound velocity profile during the sea trial. The initial distance between the two vessels was 1.1 km, with the channel response and sound velocity profile illustrated in Fig. 5(a) and Fig. 5(b), respectively, which indicates a multipath delay spread of about 3 ms and a weak positive sound velocity gradient.

The parameters of transmitted packet and initialization settings of algorithm are all identical to those of numerical simulation. Similarly, the same OFDM receiver was employed to perform OFDM demodulation, and the generated BER results were used for performance evaluation.

During the sea trial experiment, ten continuous frames of received OFDM packets were adopted for performance analysis, with the results of which displayed in Fig. 6. It could be observed from the Fig. 6(a) that the Doppler estimated by the five reference strategies exhibit similar trend, initially centering around −7 Hz and then decreasing to about −16 Hz to −14 Hz after the 6-th frame. Moreover, the Doppler results obtained by the cross-

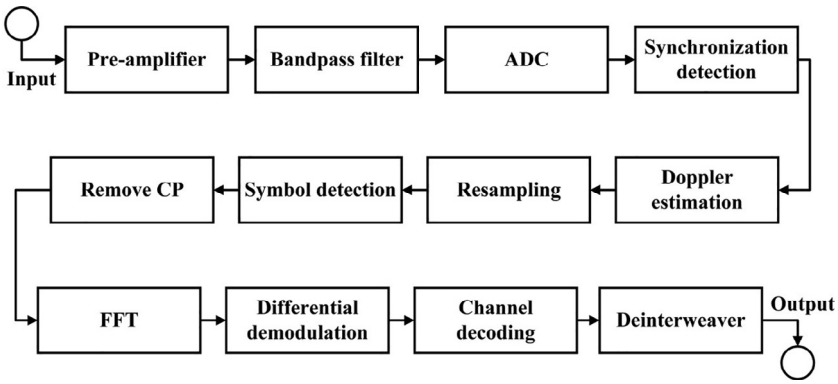

Fig. 3. Block chart of receiver.

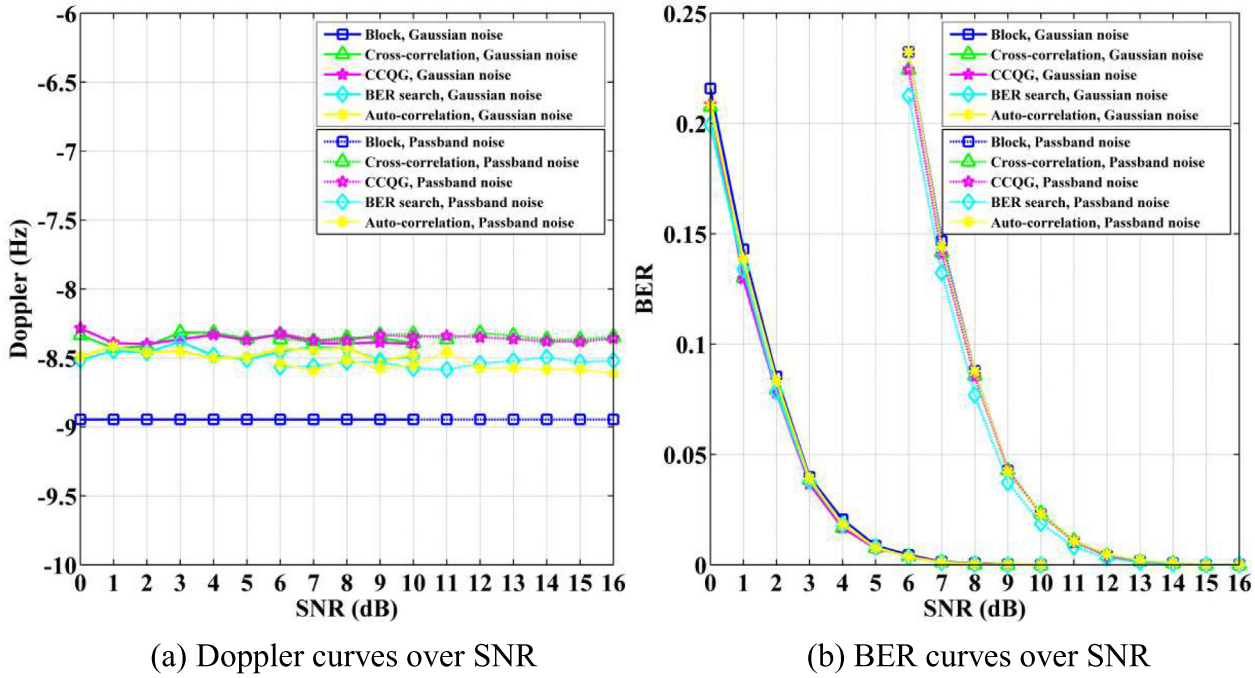

Fig. 4. The Doppler and BER with respect to SNR.

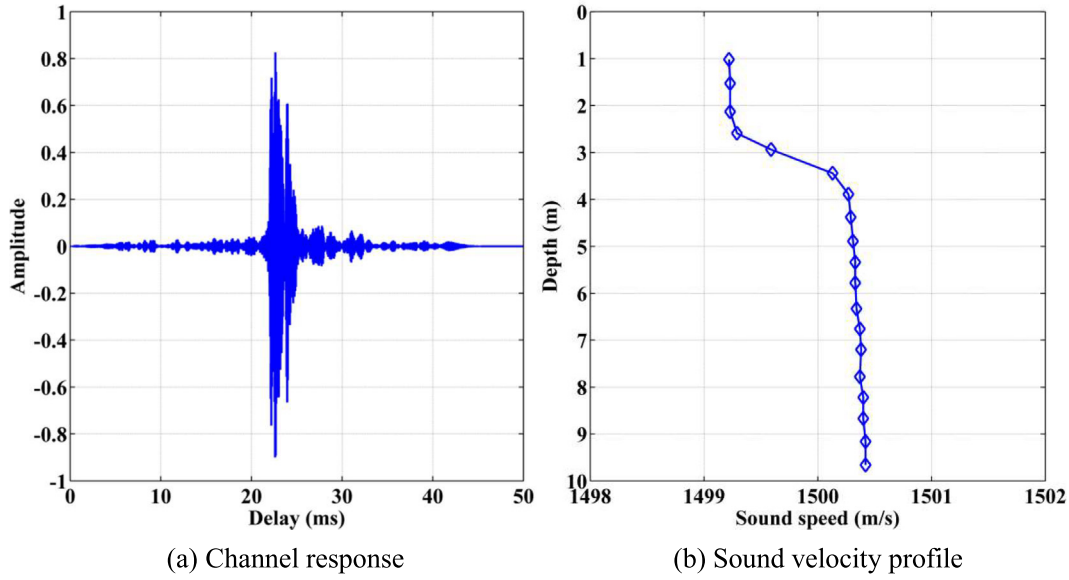

Fig. 5. Channel response and sound velocity profile.

correlation and the CCQG estimation approaches were almost the same.

After the Doppler estimation, the received packets were resampled to perform Doppler correction for OFDM demodulation, the BER curves obtained via which are displayed in Fig. 6(b). From Fig. 6(b) we can see that the block estimation, cross-correlation estimation, auto-correlation estimation, BER search estimation and the proposed CCQG estimation approaches similarly correspond to a near-zero or zero BER behavior for the starting 5 frames. When the Doppler begins to increase after the 6-th frame, the performance of the block estimation algorithm exhibits significant degradation. Furthermore, while the BER curves of cross-correlation estimation, auto-correlation estimation, BER search estimation and the CCQG estimation strategies also tend to increase, the BER search method remains the slightest performance loss with the rising of Doppler.

From the numerical simulations and sea trial experiments we can see that the BER search estimation algorithm achieves the best BER performance due to its capability of mitigating the mismatch between Doppler estimation and bit-level demodulation. However, as the OFDM demodulation process needs to be repeatedly performed to produce BER for pursuing the optimum match in a two-dimensional search grid, high calculation amount can be caused for the BER search strategy. In addition, due to the adoption of quasi-gradient iteration designed in this paper, the CCQG algorithm is able to achieve almost the same estimation performance as that of the cross-correlation strategy while taking much less complexity. Further analysis refers to Section 3.4.

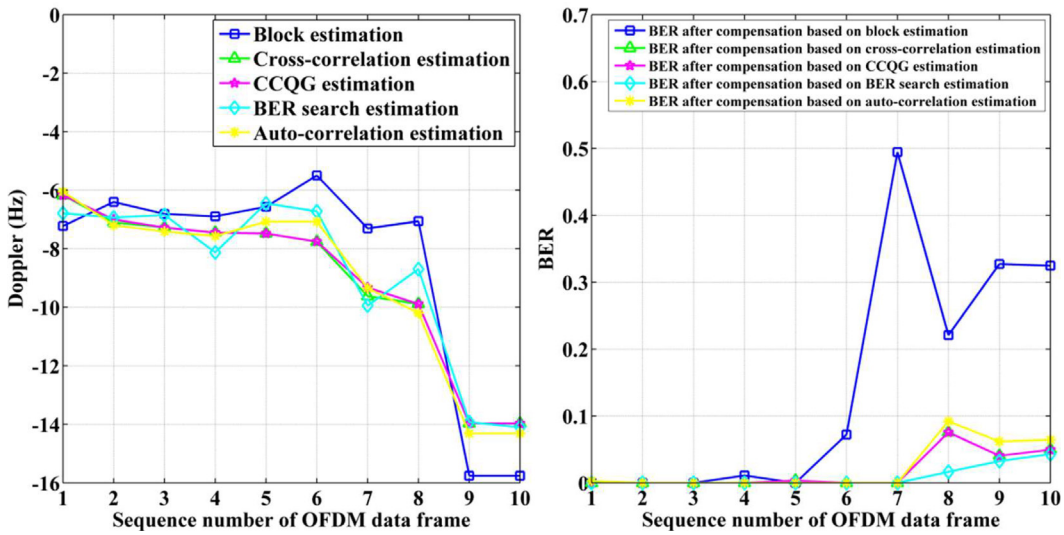

(a) Doppler with respect to OFDM data frame (b) BER with respect to different algorithms

Fig. 6. Doppler and BER over sequence number.

3.3. Impact of algorithm parameters on performance

As the evaluation accuracy of the proposed algorithm was dependent on the parameter settings distinctly, the average BER results of sea trial experiments with respect to different algorithm parameters were investigated and analyzed in Fig. 7. With three different λ of 1, 2 and 3, the resolution of fine Doppler searching interval $\Delta\varepsilon_f$ was set to 1 Hz, 0.1 Hz, 0.01 Hz and 0.001 Hz respectively for the performance analysis. From Fig. 7 we can see that, while the BER with smoothed quasi-gradient was better than that without smoothing, the parameter λ of 2 achieved the best BER behavior.

Meanwhile, as revealed in Fig. 7, while tuning of the fine Doppler searching interval only leads to slight BER behavior variations, a $\Delta\varepsilon_f$ of 0.01 seems to be reasonable in seeking a trade-off between estimation accuracy and computational complexity. Note that, when λ = 1, with the decreasing of Doppler search interval the BER even tend to rise, which may be caused by trapping into local maximum in the quasi-gradient iteration.

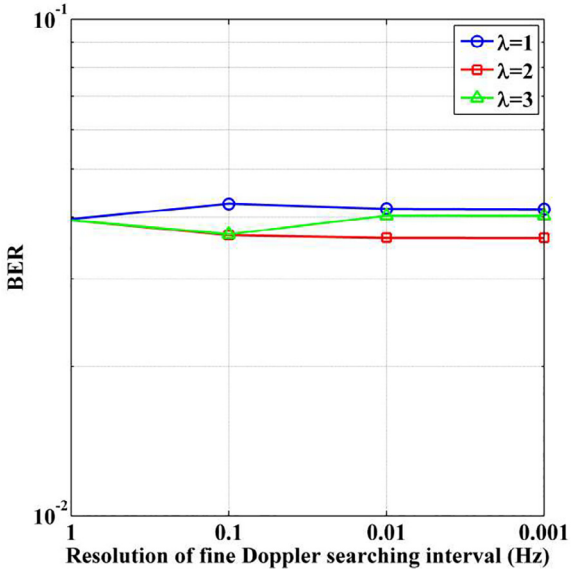

Fig. 7. BER behaviors under different parameter settings for sea trial.

3.4. Analysis of complexity and convergence

In this section, the computational complexity of the proposed CCQG algorithm, cross-correlation strategy and BER search approach was analyzed in terms of the total search times (or iterative times) as well as the additive and multiplicative calculation per search or iteration. Firstly, to facilitate performance comparison, the fixed Doppler interval $\Delta\varepsilon = 0.01$ and $\Delta\varepsilon = 0.05$ are used to calculate the grids of Doppler for cross-correlation estimation and BER search respectively, with the corresponding Doppler search range expressed as

$$floor\{\varepsilon_2 - \varepsilon_1\} = 20 \tag{20.a}$$

$$\hat{\varepsilon} = \frac{1}{2}(\varepsilon_2 - \varepsilon_1) \tag{20.b}$$

where floor is the integral function, and $\hat{\varepsilon}$ denotes the desired Doppler.

Taking the 6-th frame in the sea trial as an example, the total search times of the cross-correlation algorithm, BER search strategy and the proposed algorithm were given in Table 3. From Table 3 one might notice that, for the CCQG algorithm, only a few dozens of searching were acquired to achieve almost the same accuracy, compared to the hundreds or even thousands of searching required by direct cross-correlation search strategy and BER search approach under different searching intervals adopted.

Secondly, the additive and multiplicative calculation per search were adopted to characterize the computational complexity of cross-correlation estimation, BER search and the proposed CCQG algorithms. The detailed consequences were provided in Table 4. From Table 4 we can notice that, although the computational complexity of CCQG algorithm is about 3 times that of the cross-

Table 3
Searching times of the cross-correlation, BER search and the proposed CCQG algorithms.

Algorithm	Searching times	
	$\Delta\varepsilon = 0.01$	$\Delta\varepsilon = 0.05$
Cross-correlation	2001	401
BER search	2001	401
CCQG	37	

Table 4
Computational complexity of the CCQG estimation, cross-correlation estimation and BER search estimation algorithms.

Algorithm	Computational complexity per search	
	Multiplicative calculation	Additive calculation
Cross-correlation	$6N_f\log_2 N_f + 4$	$9N_f\log_2 N_f + 2$
BER search	$2N_f\log_2 N_f$	$3N_f\log_2 N_f + \frac{67}{256}N_f$
CCQG	$18N_f\log_2 N_f + 13$	$27N_f\log_2 N_f + 9$

Note: $N_f = 4096$ represents the length of FFT calculation.

correlation strategy, the overall calculation amount of CCQG algorithm is still far less than that of the cross-correlation strategy because it greatly reduces the number of relevant searches. The BER search approach shows the lowest computational complexity, but it requires a large number of Doppler search times. Meanwhile, the searching process includes a demodulation process, which still reflects a relatively high amount of calculation.

Furthermore, to evaluate the convergence behavior of the proposed algorithm during the gradient iteration, Doppler bias ξ is expressed as

$$\xi = \tilde{\varepsilon} - \hat{\varepsilon} \tag{21}$$

where $\tilde{\varepsilon}$ denotes the estimator in the process of iteration.

Similarly, taking the 6-th frame in the sea trial as an example, the iteration curves of the CCQG algorithm with respect to different parameters were shown in Fig. 8. From Fig. 8 one might see that the estimation accuracy with smoothed quasi-gradient was obviously better than that without smoothing, which was consistent with the results of Section 3.3. Moreover, as displayed in Fig. 8, we could also see that the parameter $\lambda = 2$ achieved the optimal balance between estimation precision and complexity.

Note that, as revealed by Fig. 8, the convergence behavior of the proposed algorithm exhibits substantial fluctuations at the beginning of iterations, which reflects the over-search trend at the initial phase of Doppler searching, i.e., initially large Doppler searching intervals lead to coarse searching pattern that may search over the optimal Doppler value several times. With the gradually decreasing of the Doppler searching interval, the convergence curve tends to approach the optimization smoothly.

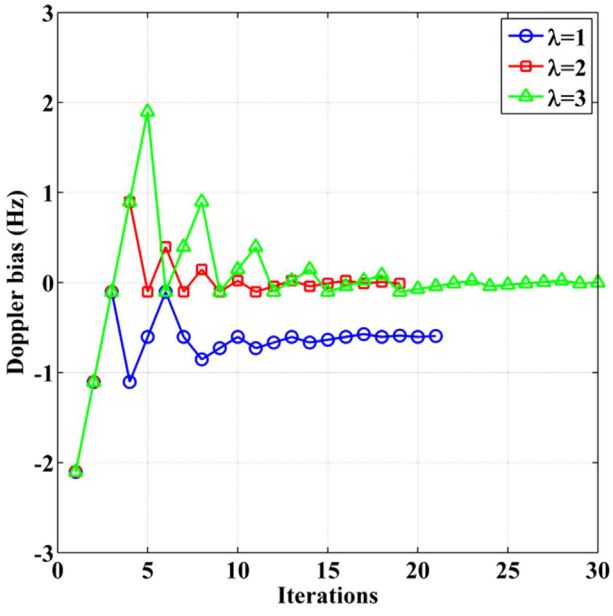

Fig. 8. The convergence behaviors of the proposed algorithm.

Meanwhile, it is evident that the Doppler bias approaches to 0 after only a couple of iterations, while achieving almost the same estimation accuracy as the direct cross-correlation approach did. Based on the above analysis, the effectiveness and superiority of the CCQG algorithm can be verified.

4. Conclusion

In this paper, a novel Doppler estimation algorithm based on cross-correlation quasi-gradient iteration is investigated for underwater acoustic OFDM communications by formulating the Doppler searching with stochastic quasi-gradient optimization. Compared with the conventional cross-correlation direct search scheme that requires a huge number of searching times, the proposed CCQG search is guided iteratively along the direction in which correlation-peak increases to pursuit the maximum correlation-peak corresponding to the desired Doppler, with much less complexity. Meanwhile, the smoothed quasi-gradient and variable Doppler interval are adopted to accelerate the convergence rate and reduce the possibility of local optimization to achieve a trade-off between the computational complexity and estimation accuracy.

Numerical simulations as well as field experiments in shallow water was provided to verify the validity and superiority of the proposed strategy in the aspect of computational complexity and estimation accuracy, compared to the conventional cross-correlation estimation, auto-correlation estimation, block estimation and BER search estimation strategies.

In view of the rapidly increasing applications of small vehicles in diverse marine missions, the proposed algorithm has the potential of being used to enable low-complexity mobile OFDM communication between small vehicles that equipped with limited computational resource.

Declaration of Competing Interest

The authors declare that they have no known competing financial interests or personal relationships that could have appeared to influence the work reported in this paper.

Acknowledgement

The authors are grateful for the funding of the National Key Research and Development Program of China (No. 2018YFE0110000), the National Natural Science Foundation of China (No.11274259 and No.11574258), and the European Union's Horizon 2020 research and innovation programme under the grant agreement number 654462 (STEMM-CCS) in support of the present research. Also the authors would like to thank Xiaokang Zhang, Ying Su, Shengqin Huang and Zhixin Liu of the College of Ocean and Earth Sciences, Xiamen University, for their assistance in sea trial, data collection and analysis.

References

[1] Perez RM, Pintado JG, Gómez AS. A real-time measurement system for long-life flood monitoring and warning applications. Sensors 2012;12(4):4213–36.
[2] Caiti A, Grythe K, Hovem JM, Jesus SM, Lie A, Munafo A, et al. Linking Acoustic Communications and Network Performance: Integration and Experimentation of an Underwater Acoustic Network. IEEE J Oceanic Eng 2013;38(4):758–71.
[3] Song A, Badiey M, McDonald VK, Yang TC. Time Reversal Receivers for High Data Rate Acoustic Multiple-Input–Multiple-Output Communication. IEEE J Oceanic Eng 2011;36(4):525–38.
[4] Felemban E, Shaikh FK, Qureshi UM, Sheikh AA, Qaisar SB. Underwater sensor network applications: a comprehensive survey. Int J Distrib Sens Netw 2015;11(11):896832. https://doi.org/10.1155/2015/896832.
[5] Petroccia R, Petrioli C, Potter J. Performance Evaluation of Underwater Medium Access Control Protocols: At-Sea Experiments. IEEE J Oceanic Eng 2017;43(2):547–56.

[6] Zhou Z, Yao B, Xing R, Shu L, Bu S. E-CARP: An Energy Efficient Routing Protocol for UWSNs in the Internet of Underwater Things. IEEE Sensors J 2015;16 (11):4072–82.
[7] Guan Q, Ji F, Liu Y, Yu H, Chen W. Distance-Vector-Based Opportunistic Routing for Underwater Acoustic Sensor Networks. IEEE Internet Things J 2019;6 (2):3831–9.
[8] Gopinath MP et al. A secure cloud-based solution for real-time monitoring and management of internet of underwater things. Neural Comput. Appl 2019;31 (1):293–308.
[9] Iqbal Z, Lee H-N. Spatially Concatenated Channel-Network Code for Underwater Wireless Sensor Networks. IEEE Trans Commun 2016;64 (9):3901–14.
[10] Ghafoor H, Noh Y, Koo I. OFDM-based spectrum-aware routing in underwater cognitive acoustic networks. IET Commun 2017;11(17):2613–20.
[11] Su Y, Fan R, Jin Z, Fu X. Design of an OFDMA-Based MAC Protocol for an Underwater Glider Network With Motion Prediction. IEEE Access 2018;6:62655–63.
[12] Li J, Zakharov YV. Efficient Use of Space-Time Clustering for Underwater Acoustic Communications. IEEE J Oceanic Eng 2018;43(1):173–83.
[13] Chunshan Liu, Zakharov YV, Teyan Chen. Doubly Selective Underwater Acoustic Channel Model for a Moving Transmitter/Receiver. IEEE Trans Veh Technol 2012;61(3):938–50.
[14] Cao X-L, Jiang W-H, Tong F. Time reversal MFSK acoustic communication in underwater channel with large multipath spread. Ocean Eng 2018;152:203–9.
[15] Jiang W, Zheng S, Zhou Y, Tong F, Kastner R. Exploiting time varying sparsity for underwater acoustic communication via dynamic compressed sensing. J Acous Soc Am 2018;143(6):3997–4007.
[16] Li J, Wang J, Wang X, Qiao G, Luo H, Gulliver TA. Optimal Beamforming Design for Underwater Acoustic Communication With Multiple Unsteady Sub-Gaussian Interferers. IEEE Trans Veh Technol 2019;68(12):12381–6.
[17] Cai J, Li Z, Hao Y, Cai J. Time-Variant Doppler Frequency Estimation and Compensation for Mobile OFDM Systems. IEEE Trans Consumer Electron 2006;52(2):336–40.
[18] Yerramalli S, Mitra U. Optimal Resampling of OFDM Signals for Multiscale–Multilag Underwater Acoustic Channels. IEEE J Oceanic Eng 2011;36 (1):126–38.
[19] Jiang X, Zeng W-J, Li X-L. Time delay and Doppler estimation for wideband acoustic signals in multipath environments. J Acoust Soc Am 2011;130 (2):850–7.
[20] Sharif BS, Neasham J, Hinton OR, Adams AE. A computationally efficient Doppler compensation system for underwater acoustic communications. IEEE J Oceanic Eng 2000;25(1):52–61.
[21] Zheng S, Tong F, Li B, Tao Q, Song A, Zhang F. Design and evaluation of an acoustic modem for a small autonomous unmanned vehicle. Sensors 2019;19 (13):1–12.
[22] H. Susako, "Method of high-resolution frequency measurement for pulse-Doppler sonar," *IEEE ISUT 2002*, Tokyo, Japan, 39-44.
[23] Kay SM, Doyle SB. Rapid estimation of the range-doppler scattering function. IEEE Trans Signal Process 2003;51(1):255–68.
[24] Abdelkareem AE, Sharif BS, Tsimenidis CC. Adaptive time varying doppler shift compensation algorithm for OFDM-based underwater acoustic communication systems. Ad Hoc Netw 2016;45:104–19.
[25] Li J, Zakharov YV, Henson B. Multibranch Autocorrelation Method for Doppler Estimation in Underwater Acoustic Channels. IEEE J Oceanic Eng 2018;43 (4):1099–113.
[26] Wan L, Wang Z, Zhou S, Yang TC, Shi Z. Performance comparison of Doppler scale estimation methods for underwater acoustic OFDM. J Electr Comput Eng 2012;2012:1–11.
[27] Zhang X, Han X, Yin J, Sheng X. Study on Doppler effects estimate in underwater acoustic communication. J Acoust Soc Am 2013;133(5):1–7.
[28] Y. M. Aval, and M. Stohanovic, "Partial FFT demodulation for coherent detection of OFDM signals over underwater acoustic communication," *IEEE OCEANS 2013*, Bergen, Norway, 1-4.
[29] Li B, Zheng S, Tong F. Bit-error rate based Doppler estimation for shallow water acoustic OFDM communication. Ocean Eng 2019;182:203–10.
[30] Tadayon A, Stojanovic M. Low-Complexity Superresolution Frequency Offset Estimation for High Data Rate Acoustic OFDM Systems. IEEE J Oceanic Eng 2019;44(4):932–42.
[31] Zakharov YV, Morozov VP. Experimental study of an underwater acoustic communication system with pseudonoise signals. *Acoust. Phys.* 1994;40 (5):707–15.
[32] T. Yao, W. Zhao, Q. Zhang, and Y. Kou, "Estimation of Doppler-shift based on correlation-peak waveform," *IEEE ICCAS 2007*, Kokura, Japan, 99-102.
[33] Zakharov YV, Morozov AK. OFDM Transmission Without Guard Interval in Fast-Varying Underwater Acoustic Channels. IEEE J Oceanic Eng 2015;40 (1):144–58.
[34] Ermoliev Y. stochastic quasigradient methods and their application to system optimization †. Stochastics 1983;9(1-2):1–36.
[35] Peeta S, Zhou C. Stochastic quasi-gradient algorithm for the off-line stochastic dynamic traffic assignment problem. Transp Res Part B: Methodol 2006;40 (3):179–206.
[36] Bykov VI, Starostin IE. Quasi-gradient models of the dynamics of closed chemical systems. Russ J Phys Chem B 2012;6(1):33–7.
[37] Li P, Jin B, Wang D, Zhang B. Distribution System Voltage Control Under Uncertainties Using Tractable Chance Constraints. IEEE Trans Power Syst 2019;34(6):5208–16.
[38] Zhu Hu, Deng L. Image matching using Gradient Orientation Selective Cross Correlation. Optik 2013;124(20):4460–4.
[39] Zakharov YV, Li J. Autocorrelation method for estimation of Doppler parameters in fast-varying underwater acoustic channels. In: The 3rd Underwater Acoustics Conference & Exhibition, Island of Crete, Greece. p. 21–6.
[40] Wan L, Jia H, Zhou F, Muzzammil M, Li T, Huang Yi. Fine Doppler scale estimations for an underwater acoustic CP-OFDM system. Signal Process 2020;170:107439. https://doi.org/10.1016/j.sigpro.2019.107439.
[41] Baosheng Li, Shengli Zhou, Stojanovic M, Freitag L, Willett P. Multicarrier Communication Over Underwater Acoustic Channels With Nonuniform Doppler Shifts. IEEE J Oceanic Eng 2008;33(2):198–209.
[42] Sen S, Nehorai A. Adaptive Design of OFDM Radar Signal With Improved Wideband Ambiguity Function. IEEE Trans Signal Process 2010;58(2):928–33.
[43] Gu Y, Tang K, Cui H. LMS Algorithm With Gradient Descent Filter Length. IEEE Signal Process Lett 2004;11(3):305–7.
[44] Stojanovic M. Retrofocusing techniques for high rate acoustic communications. J Acoust Soc Am 2005;117(3):1173–85.
[45] Stojanovic M, Preisig J. Underwater acoustic communication channels: Propagation models and statistical characterization. IEEE Commun Mag 2009;47(1):84–9.
[46] Haas E, Kaiser S. Two-dimensional differential demodulation for OFDM. IEEE Trans Commun 2003;51(4):580–6.